Scientific Report to the NERC Geophysical Equipment Facility
SEIS-UK loan for:
Afar Rift Consortium (Sept, 2007 - Oct, 2009)

Graham Stuart[1], James Hammond[2], Mike Kendall[2], Derek Keir[1,3]
[1]School of Earth and Environment, University of Leeds, Leeds, LS2 9JT; [2]School of Earth Sciences, University of Bristol, Bristol; [3]National Oceanography Centre, Southampton.

Abstract

SEIS-UK provided an initial loan of 27 broadband seismic systems (23 x CMGESP, 3 x CMG3T and 1 CMG6TD) for a period of between 16 and 24 months, for deployment in a network that extended more than 500 km across northern Ethiopia, centred on the Afar Depression. The SEIS-UK deployment was coeval with an NSF funded deployment of 14 CMG40T seismometers in the central part of Afar. The initial network ran from September 2007 until October 2009. These systems recorded continuously at 50Hz with relatively minor data losses due to equipment problems. All data have been archived with IRIS (Incorporated Research Institutions for Seismology) and is a key dataset in the NERC Afar Consortium Project. Teleseismic tomography has been used to deliver P- and S-wave velocity models for the upper mantle. These show focussed, melt related, anomalies in the top 100km of the lithosphere with broad upwellings below. Crustal structure across Afar and on the Western Plateau are constrained with P-wave receiver functions and surface wave dispersion, providing understanding on the breakup history of Afar and showing that the lower crust contains large amounts of melt. S-wave receiver functions show that the lithosphere beneath Afar has been largely destroyed and that melting begins at depths requiring little thermal anomaly. Measurements of seismic anisotropy from splitting of SKS-waves and local earthquake S-wave data show that melt dominates the anisotropy in the crust and lithosphere beneath the magmatic segments, while flow in the mantle provides an additional anisotropic fabric at depth. The local seismicity, associated with the continued dyke intrusion, has been studied in detail by our University of Rochester (USA) collaborators led by Prof. Cindy Ebinger. This seismicity has provided unprecedented detail on 14 dike intrusions into the crust following the main dike in September 2005. Local and regional earthquakes have also been used to produce surface wave velocity maps of the crust, and Pn tomographic images of the uppermost mantle showing that melt is predominantly focussed at the magmatic segments. All these results have been presented at international conferences and have been and are currently being written up for leading international journals.

Background

The Afar Depression (Figure 1) marks the intersection of the southern Red Sea rift (RSR), the Gulf of Aden rift (GOA) and the Main Ethiopian Rift (MER), forming an archetypal rift-rift-rift triple junction (e.g. McKenzie et al., 1972). The Afar rifts are the most mature part of the continental East-Africa Rift system and hosts the on-shore extension of the Red Sea and Gulf of Aden oceanic spreading (e.g. Beyene and Abdelsalam, 2005). They are the only place on the planet where the transition from late-stage continental rifting to oceanic seafloor spreading is occurring subaerially today, and it is occurring above Earth's youngest mantle plume (e.g., Hayward and Ebinger, 1996).

Recent active rifting and dike injection has focused scientific attention on this area (Ebinger et al., 2010). In September 2005, a 60km long segment of the Dabbahu-Manda-Hararo (DMH) rift segment opened in two weeks (Wright et al., 2006), and geodetic and seismic monitoring, using data mainly from this experiment, have revealed 14 episodes of dike injection along this segment of the rift (e.g. Wright et al., 2006, Ayele et al., 2009, Hamling et al., 2009, Belachew et al., 2011}.

Survey Procedure

The 14 seismometers of the NSF project were localised around the Dabbahu rift segment with the objective of investigating the on-going seismicity associated with dyking. The 27 NERC seismometers covered a much larger aperture (Fig 1), thus providing data to study crust and upper mantle earth structure, and determine the underlying dynamics of rifting in the region. The SEIS-UK Afar network was designed to; a) cover a large aperture, with regular spacing for tomography and seismicity studies; b) contain cross rift profiles to enable receiver functions to constrain the variation in crust and lithospheric structure across the rift, c) use CMG-3T stations on the edge of the array to maximise long inter-station paths used for surface wave studies, d) provide long-term monitoring of seismic anisotropy and seismicity. The seismicity around the DMH segment continues to be monitored in Afar on a reduced 12 station SEIS-UK network as of Oct 2009 to present (Oct 2011).

Help and collaboration from Addis Ababa University (in particular Dr Atalay Ayele), the regional Afar government, the Federal Ethiopian Government and SEIS-UK employees was essential for the success of the project. Logistical procedures were already well-advanced following the 2005 NERC funded Urgency Array in Afar. We located stations in fenced compounds to maximise security. Care was taken to achieve a regular spacing of stations, but not at the expense of finding a secure location. Available locations were mainly limited to towns with a fenced government compounds (e.g., school, clinic, office). In south-east and east Afar, security and the presence of access roads was a problem. This resulted in a poorer than desired station distribution in this region (Figure 1). See Table 1 for station details.

A hole ~1m deep, ~0.7m in diameter, was dug at the site to house the seismometer. The stations on the western plateau were constructed with a sand layer at the base of the hole with a level slab on top of the sand. The seismometer was then placed on top, levelled and aligned with magnetic north, and the firewire and sensor cable attached. An upturned bin was then placed surrounding the slab and seismometer to provide insulation. This hole was then back filled with the soil removed from the hole. This construction was changed for the remaining stations on the advice of SEIS-UK, where the seismometer was placed in a plastic bag and buried directly in the soil, removing the upturned bin. In central Afar the sensor pits were protected from the heat using buried reflective sheets.

A second hole close to the seismometer hole was dug, and a plastic bin placed inside. This was of a depth so that the bin was ~20cm above the surface. The battery, break out box, and in the case of the CMG3T, the Taurus data-logger, were placed in this box with all cables attached. Cables for the sensor and firewire led from this box to the seismometer hole. Cables for the GPS and solar panels led out of the box and connected with the solar panels and GPS antenna located nearby. All cables out of the box were fed through flexible plastic conduit and secured to posts or buried. The battery/cable box was then covered with insulation and plastic, and secured with tape. Before the box was secured the configuration of the sensors was checked using the palms for the ESP instruments and the Taurus data logger in the case of the CMG-3T instruments.

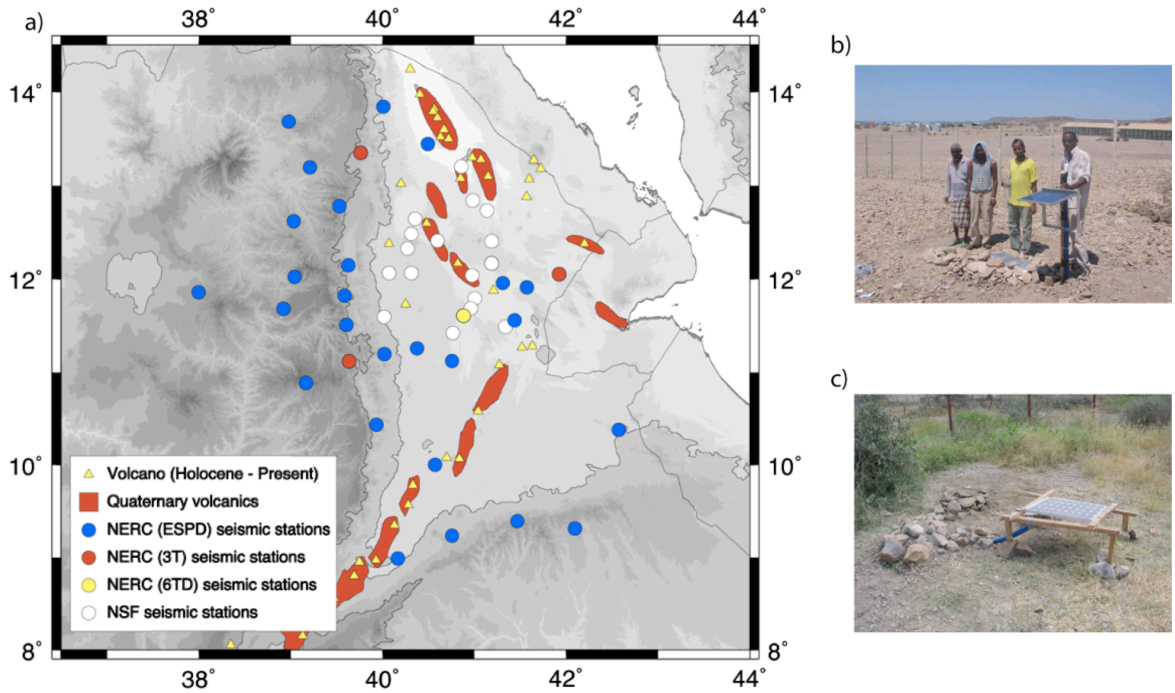

Figure 1. a) Distribution of broadband stations used in this study, b) Typical ESPD/6TD deployment, c) typical 3T deployment.

Data Quality

The ESP systems were primarily used in this deployment. They were generally easy to use, especially to anyone familiar with Guralp's previous systems. The data were of excellent quality (Figure 2) and of lower noise than the 3T systems when utilised in temporary deployments with no bedrock. The only problem we encountered (after some initial firmware problems which Guralp fixed) was that some of the instruments seem to have trouble locking at the end of the deployment, even if the station was otherwise working fine. This only occurred in the Afar stations, suggesting a possible correlation with heat (temperatures regularly exceed 50C); further analysis is needed to confirm this. The 3T systems worked well, although some horizontal components stopped working

Station Code	Location	Sensor	Sensor ID	Latitude (°)	Longitude (°)	Elevation (m)	Date(Julian Day) Time	Date(Julian Day) Time	Sample rate (Hz)
ABAE	Abala	3T	T34881	13.354	39.764	1447	2007.281 06:00:00	2009.284 10:00:00	50
ADTE	Adaitu	3ESP	T34601	11.122	40.757	506	2007.294 06:00:00	2009.290 14:00:00	50
ADYE	Abi_Adi	3ESP	T34510	13.635	38.981	1860	2007.282 07:00:00	2009.282 13:00:00	50
AKEE	Akesta	3ESP	T34597	10.888	39.168	3235	2007.278 07:00:00	2009.279 13:00:00	50
ASYE	Asayita	6T	T6108	11.561	41.442	370	2008.068 04:00:00	2008.132 05:00:00	20
ASYE	Asayita	3ESP	T34977	11.561	41.442	370	2008.132 05:00:00	2009.282 12:00:00	50
AWSE	Awash	3ESP	T34660	8.990	40.170	921	2008.138 06:00:00	2009.277 12:00:00	50
BOBE	Biye Kabobe	3ESP	T34752	10.380	42.572	941	2009.053 00:00:00	2009.279 09:00:00	50
BTIE	Bati	3ESP	T34573	11.195	40.022	1659	2007.278 06:00:00	2009.285 14:00:00	50
DERE	Dese	3T	T34880	11.118	39.635	2545	2007.276 06:00:00	2009.278 15:00:00	50
DICE	Di Choto	3ESP	T34599	11.914	41.574	464	2007.291 06:00:00	2009.281 15:00:00	50
ELLE	Elwoha	3ESP	T34623	11.258	40.378	672	2007.293 08:00:00	2009.285 16:00:00	50
ERTE	Kuso Wad	3ESP	T34849	13.446	40.497	-5	2008.134 06:00:00	2008.279 03:00:00	50
ERTE	Kuso Wad	3ESP	T34976	13.446	40.497	-5	2008.279 03:00:00	2009.292 12:00:00	50
GASE	Gashena	3ESP	T34591	11.681	38.921	2972	2007.285 10:00:00	2009.280 11:00:00	50
GEWE	Gewane	3ESP	T34739	10.005	40.574	572	2007.295 06:00:00	2009.280 10:00:00	50
HALE	Berhale	3ESP	T34660	13.842	40.008	710	2008.073 07:00:00	2008.130 07:00:00	50
HALE	Berhale	3ESP	T35482	13.842	40.008	722	2008.130 07:00:00	2009.282 12:00:00	50
HYNE	Harar	3ESP	T34398	9.315	42.096	1982	2007.299 06:00:00	2009.278 12:00:00	50
KOBE	Kobo (Dese)	3ESP	T34732	12.151	39.630	1508	2007.279 08:00:00	2009.280 12:00:00	50
KORE	Kare Kore	3ESP	T34752	10.427	39.934	1774	2007.287 07:00:00	2009.051 00:00:00	50
LALE	Lalibela	3ESP	T34564	12.026	39.038	2422	2007.285 04:00:00	2009.280 14:00:00	50
LYDE	Elidar	3T	T34879	12.055	41.926	435	2007.292 06:00:00	2009.059 12:00:00	50
LYDE	Elidar	6T	T6058	12.055	41.926	435	2009.059 12:00:00	2009.281 12:00:00	25
MAYE	Maychew	3ESP	T34589	12.783	39.534	2440	2007.280 05:00:00	2009.280 16:00:00	50
MISE	Meiso	3ESP	T34670	9.237	40.759	1310	2007.297 08:00:00	2009.277 16:00:00	50
QATE	Kobo (Harar)	3ESP	T34736	9.375	41.469	2148	2007.298 07:00:00	2009.278 10:00:00	50
SEKE	Sekota	3ESP	T34636	12.622	39.033	2264	2007.284 06:00:00	2009.281 16:00:00	50
SISE	Harsis	6T	T6108	11.607	40.884	454	2008.132 07:00:00	2009.060 12:00:00	20
SMRE	Semre	3ESP	T34731	13.198	39.211	1977	2007.283 04:00:00	2009.282 09:00:00	50
SRDE	Serdo	3ESP	T34662	11.958	41.310	392	2007.294 06:00:00	2009.281 17:00:00	50
WLDE	Waldiya	3ESP	T34660	11.824	39.587	1879	2007.279 05:00:00	2008.071 10:00:00	50
WUCE	Wuchale	3ESP	T34569	11.512	39.606	1912	2007.277 06:00:00	2009.064 00:00:00	50
YAYE	Debre Tabor	3ESP	T34569	11.861	37.997	2627	2009.067 12:00:00	2009.279 17:00:00	50

Table 1: Afar consortium seismic network: Station details.

towards the end of the deployment (see field report, http://www.le.ac.uk/seis-uk/downloads/Afar_NERC_field_report.pdf for details). The Taurus data logger was very easy to use in the field. The one 6TD system was primarily used as a spare and generally worked well (it was swapped during the deployment due to some download problems related to the firewire cable.

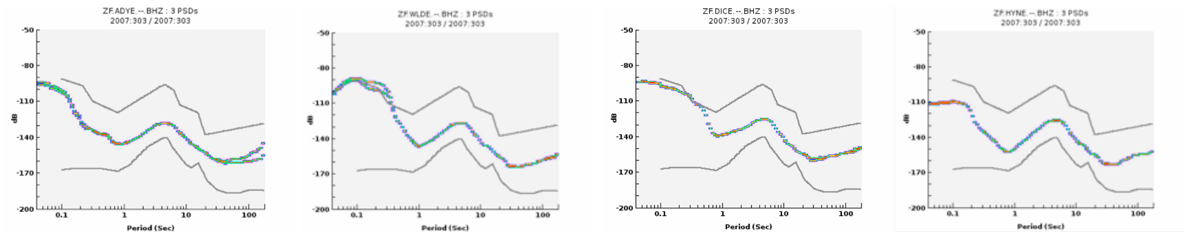

Figure 2. Power spectral density plots of the vertical components over a seismically quiet period. The stations show typical ambient noise at 4 ESPD stations across the array, from northwest (ADYE) and western plateau (WLDE), Afar (DICE) and the southeastern plateau (HYNE). The black lines show the high and low noise model of Peterson (1993). The model value is shown as a coloured line.

Processing

We used the SKS analysis technique by Teanby et al., (2004), to determine fast polarization directions for crustal (Fig. 3a) and mantle shear-wave anisotropy (Fig. 3b). Rayleigh wave group velocity tomography (Guidarelli et al. 2011) was used to determine the shear wave velocity of the crust (Fig 4a) and a procedure after Seward et al (2009) Pn velocity distribution (Fig 4b). The methodology of VanDecar et al., (1995) was applied to invert for relative travel times and determine P- and S-wave upper mantle velocity models (Figure 4c & 4d). We use the extended time multi-taper receiver function technique of Helffrich 2006 to generate P- and S-wave recieiver functions (Fig. 5). Additionally, in collaboration with our University of Rochester partners (Belachew et al, 2011), we use standard earthquake location procedures to accurately locate earthquakes in the Afar Depression.

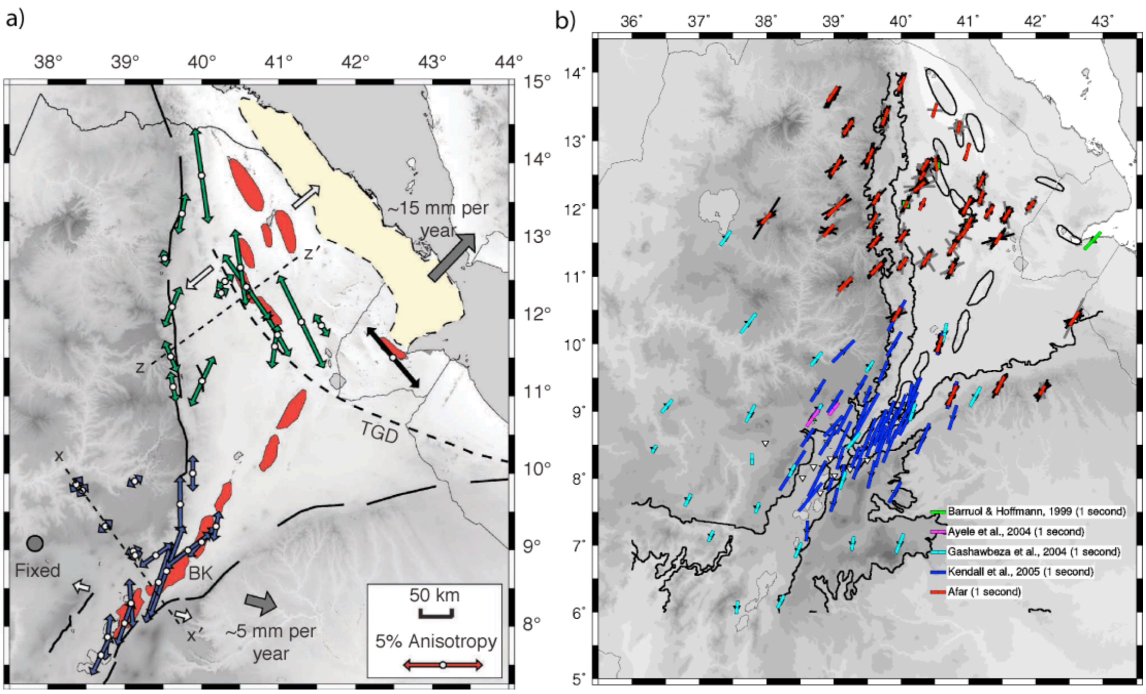

Figure 3. a) Crustal (Keir et al., 2011) and b) upper mantle anisotropy (Hammond et al., in prep) as indicated by local and SKS fast polarization directions respectively. Arrows are oriented in the direction of the fast shear-wave polarization and are proportional to anisotropy magnitude (local) and delay time (SKS).

Interpretation and preliminary findings

The combination of seismic techniques utilised in this project have enabled us to produce well-constrained images of both P- and S-wave velocity through the crust to the base of the manlte transition zone. Seismicity studies show that earthquakes at DMH originate at a central magma chamber and propagate north and south during dyking episodes (Ayele et al., 2009, Belachew et al., 2011). Shear-wave splitting based on local Afar earthquakes show that crustal strain is highest at the magmatic segments, and likely influenced by melt (Fig. 3) (Keir et al., 2011). Thus, magma injection into the crust accommodates a large part of strain during rifting episodes. This is further supported by images of crustal S-wave velocity from surface wave group velocity inversions (Guidarelli et al., 2011 in review). These show extremely low velocities in the crust beneath the recently active DMH and Erta Ale segments (Fig. 4).

The low velocities persist to lower crustal depths (Guiderelli et al., 2011 in review), and this observation is supported by high Vp/Vs determined by receiver functions (Hammond et al., 2011) (Fig. 5). These high Vp/Vs are seen primarily where crust has been thinned, showing that melt ponds preferentially in these regions. This thin crust is primarily evident west of the current rift axis, suggesting that the Red Sea Rift has migrated eastwards over time (Hammond et al., 2011).

At the base of the crust Pn tomography shows low velocities again below the magmatic segments (Stork et al., 2011 submitted) suggesting the melt remains focussed beneath the rift segments into the mantle. P-wave and S-wave relative travel time tomography shows focussed melt related anomalies extending down to ~100km (Hammond et al., in prep), and depth of melt initiation is further constrained by S-wave receiver functions (~75km) (Rychert et al., 2011 in review). This melt provides an anisotropic signature, which can be observed in SKS-wave splitting (Hammond et al., in prep).

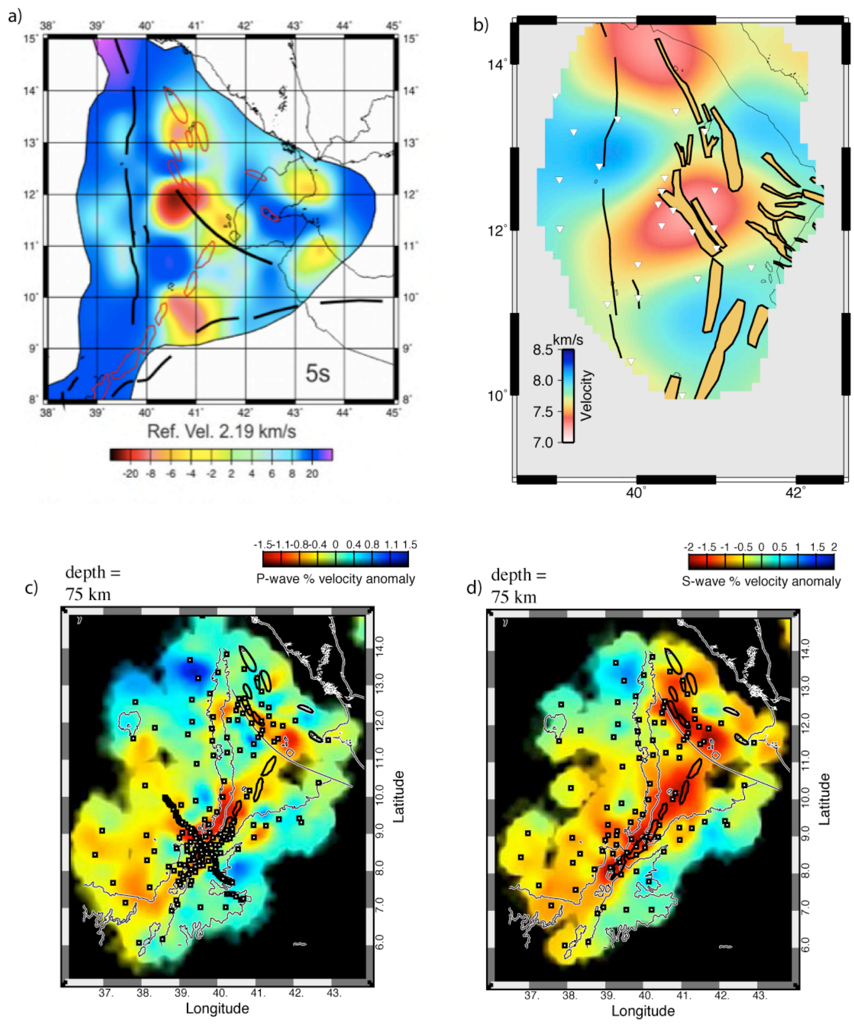

Figure 4. a) Group velocities based on surface-wave inversions at 5s period (Guidarelli et al. 2011, submitted) b) Pn velocity model for Afar (Stork et al. 2011, submitted) c) Depth slices through the P-wave tomographic model and d) depth slices through the S-wave model at 75km depth (Hammond et al., in prep.)

Below ~100km, P- and S-wave tomography inversions show broader anomalies, with flow (constrained from SKS-wave splitting measurements) in a NE/SW direction, suggesting that a compositional or thermal anomaly is more diffuse and possibly flows along lithospheric topographic gradients. In the mantle transition zone, however, more focussed anomalies are observed, suggesting a complicated upwelling and no evidence for a narrow conduit, plume-like anomaly (Hammond et al., in prep).

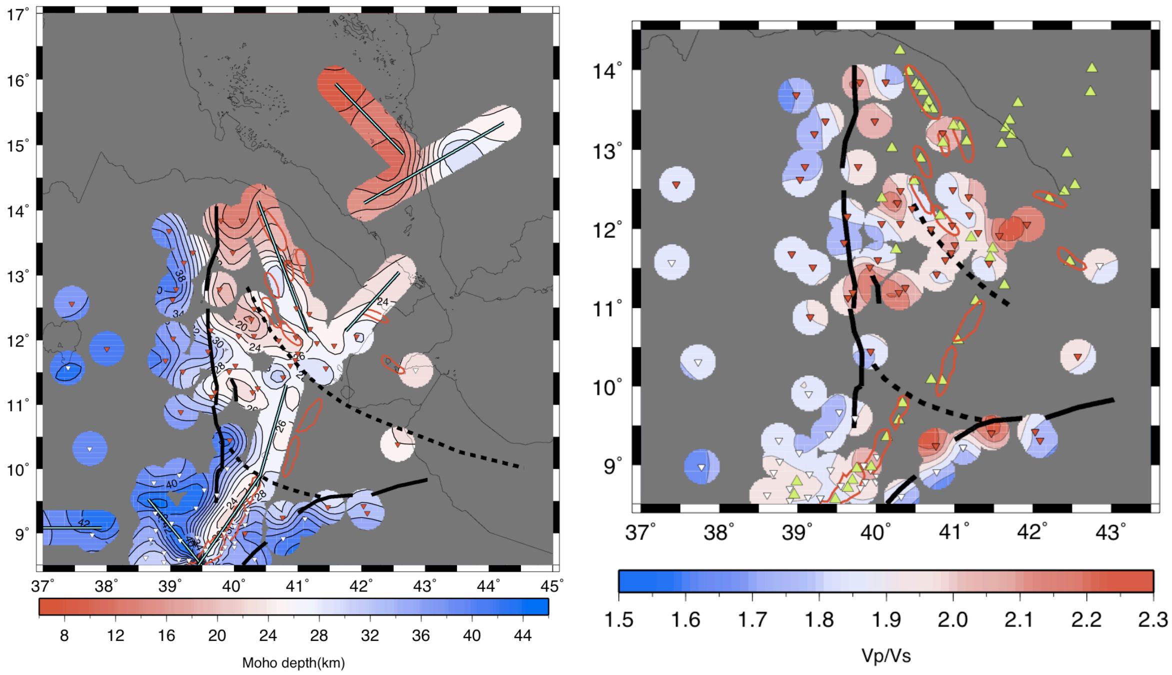

Figure 5. a) Map showing crustal thickness variations and b) bulk crustal Vp/Vs across northern Ethiopia. Dashed lines show the Arcuate Accommodation zone (southern line) and Tendaho-Goba Discontinuity (northern line). Solid lines show border faults, green triangles show volcanoes, red triangles show station locations and red lines show quartenery magmatic segments (After Hammond et al., 2011).

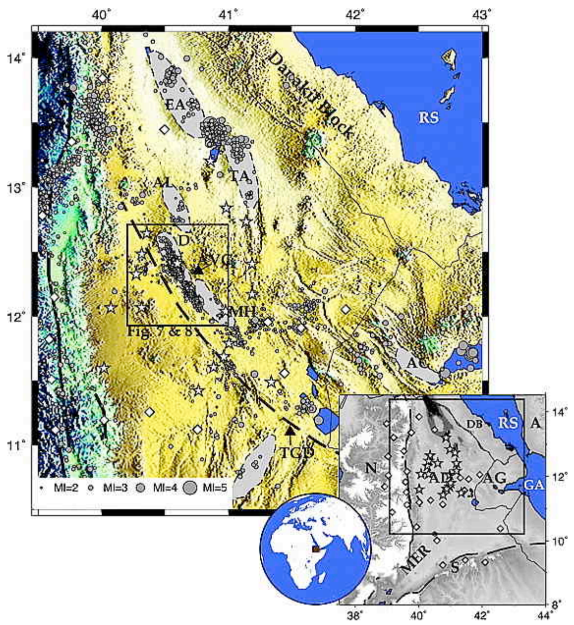

Figure 6. Seismicity of the Afar Depression (grey circles) recorded between 2007 and 2009 on the combined IRIS-PASSCAL (stars) and Seis-UK (diamonds) seismic network shown the in the inset after Belachew et al 2011.

Conclusions and recommendations

This SEIS-UK loan has enabled the collection of a high quality dataset covering one of the least accessible parts of the world. 27 stations were operated safely and continuously for between 16-24 months. No stations were lost or damaged during the deployment. Seismicity, local shear-wave splitting, P- and S-wave receiver functions, Pn tomography, and surface wave studies have all been completed (published or in review). Other studies are well established and will soon follow (P- and S-wave tomography, seismic noise interferometry, transition zone receiver functions). Additionally, extensions to this original network mean data are still being collected in both Ethiopia and Eritrea. These data will improve the monitoring of the region (e.g. Nabro Volcano, Erta Ale volcanic range, Dallol), and also improve coverage for all the seismic imaging techniques discussed here.

The Afar region is the perfect natural laboratory to study the final stages of continental breakup, a major objective of the Afar Rift Consortium project. The dataset has helped to provide accurate earthquake locations, helping understand dyke propagation processes, and determine earthquake/volcanic hazard in the region. The range of imaging techniques applied have allowed us to trace the melt migration pathways from its generation at ~75km depth to its eruption at the surface at the DMH or Erta Ale segments. P- and S-wave models of crust and upper mantle structure have also increased our understanding of the dynamic processes under the Afar Depression.

Publications

Belachew, M., C. Ebinger, D. Coté, D. Keir, J. V. Rowland, J. O. S. Hammond, and A. Ayele (2011), Comparison of dike intrusions in an incipient seafloor-spreading segment in Afar, Ethiopia: Seismicity perspectives, J. Geophys. Res., 116, B06405, doi:10.1029/2010JB007908.

Ebinger, C., A. Ayele, D. Keir, J. Rowland, G. Yirgu, T. Wright, M. Belachew and I. Hamling (2010), Length and timescales of rift faulting and magma intrusion: The Afar rifting cycle from 2005 to present. Annual Review of Earth and planetary Sciences 38:437-64 doi:10.1146/annurev-earth-040809-152333.

Guidarelli, M., G. W. Stuart, J. O. S. Hammond, J-M. Kendall, A. Ayele and M. Belachew (in review), Surface wave tomography across Afar, Ethiopia: locating regions of magma intrusion in the crust, Geophys. Res. Lett.

Hammond, J. O. S., J-M. Kendall, G. W. Stuart, D. Keir, C. Ebinger, A. Ayele and M. Belachew (2011), The nature of the crust beneath the Afar triple junction: evidence from receiver functions, Geochem. Geophys. Geosys.

Hammond, J. O. S. et al., (in prep), Flow, Fossil or Fluid; unraveling seismic anisotropy beneath Afar, Ethiopia

Hammond, J. O. S. et al., (in prep), Upper mantle velocity structure beneath the Afar triple junction.

Keir, D., M.Belachew, C.Ebinger, J-M.Kendall, J. O. S. Hammond, G. Stuart, A. Ayele and J. Rowland (2011), Mapping the evolving strain field during continental breakup from crustal anisotropy in the Afar depression. Nature Communications, DOI: 10.1038/ncomms1287

Rychert, C. A., J. O. S. Hammond, J-M. Kendall, N. Harmon, D. Keir, C. Ebinger, A. Ayele, I. Bastow, G. Stuart, M. Belachew, Seismically Imaging the Destruction of Continental Lithosphere beneath Afar (in press to Nature Geoscience)

Stork, A., G. Stuart, C. Henderson, D. Keir and J. Hamond., Uppermost mantle (Pn) velocity model for the Afar region, Ethiopia: An insight into rifting processes (submitted to GRL).

Other conference presentations describing the results of the Afar Rift Consortium project have been made at 2007-2011 American Geophysical Union Fall meetings in San Francisco, as well as other small meetings such as Asmara Geocongress, Frontiers of Seismology, New Advances in Geophysics, IASPEI meeting ….

Other References:

Ayele, A., D. Keir, C. Ebinger, T. J. Wright, G. W. Stuart, W. R. Buck, E. Jacques, G. Ogubazghi, and J. Sholan (2009), September 2005 mega-dike emplacement in the Manda-Harraro nascent oceanic rift (Afar depression), Geophys. Res. Lett., 36, l20306,doi:10.1029/2009GL039605.

Beyene, A., and M. G. Abdelsalam (2005), Tectonics of the Afar Depression: A review and synthesis, J. Afr. Earth Sci., 41, 41–59.

Hamling, I., A. Ayele, L. Bennati, E. Calais, C. Ebinger, D. Keir, E. Lewi, T. Wright, and G. Yirgu (2009), Geodetic observations of the ongoing Dabbahu rifting episode: new dyke intrusions in 2006 and 2007, Geophys. J. Int., 178 (2), 989–1003.

Hayward, N. J., and C. J. Ebinger (1996), Variations in along-axis segmentation of the Afar rift system, Tectonics, 15 (2), 244–257.

Helffrich, G. (2006), Extended-time multi-taper frequency domain cross-correlation receiver function estimation, Bull. Seism. Soc. Am, 96, 344–347.

McKenzie, D. P., D. Davies, and P. Molnar (1972), Plate tectonics of the Red Sea and East Africa, Nature, 224, 125–133.

Peterson, J., 1993. Observation and modeling of seismic background noise, U.S. Geol. Surv. Open File Rep., 93–322, 1–95.

Seward, A.M., C.M. Henderson and E.G.C. Smith (2009),Models of the upper mantle beneath the central North Island, New Zealand, from speeds and anisotropy of subhorizontal P waves (Pn), *J. Geophys. Res. 114*, B0131, doi:10.1029/2008JB005805.

Teanby, N. A., J.-M. Kendall, and M. Van der Baan, Automation of shear–wave splitting mea- surements using cluster analysis, Bull. Seis. Soc. Am., 94, 453–463, 2004.

VanDecar, J. C., D. E. James, and M. Assumpc¸a˜o, Seismic evidence for a fossil mantle plume beneath South America and implications for plate driving forces, Nature, 378, 25–31, 1995.

Wright, T., C. Ebinger, J. Biggs, A. Ayele, G. Yirgu, D. Keir, and A. Stork (2006), Magma-maintained rift segmentation at continental rupture in the 2005 Afar dyking episode, Nature, 442 (7100), 291–294.